2D Teager-Kaiser Energy Operator for the translation motion compensation in ISAR signatures

Jean-Christophe Cexus, Ali Khenchaf

▶ **To cite this version:**

Jean-Christophe Cexus, Ali Khenchaf. 2D Teager-Kaiser Energy Operator for the translation motion compensation in ISAR signatures. 9th International Symposium on Signal, Image, Video and Communications - ISIVC'2018, Nov 2018, Rabat, Morocco. hal-01977996

HAL Id: hal-01977996

https://ensta-bretagne.hal.science/hal-01977996

Submitted on 11 Jan 2019

HAL is a multi-disciplinary open access archive for the deposit and dissemination of scientific research documents, whether they are published or not. The documents may come from teaching and research institutions in France or abroad, or from public or private research centers.

L'archive ouverte pluridisciplinaire **HAL**, est destinée au dépôt et à la diffusion de documents scientifiques de niveau recherche, publiés ou non, émanant des établissements d'enseignement et de recherche français ou étrangers, des laboratoires publics ou privés.

2D Teager-Kaiser Energy Operator for the translation motion compensation in ISAR signatures

Jean-Christophe Cexus, Ali Khenchaf
ENSTA Bretagne - Lab-STICC, UMR CNRS 6285
2, Rue François Verny, 29806 Brest Cedex 9, France.
Email: {jean-christophe.cexus, ali.khenchaf}@ensta-bretagne.fr

***Abstract*—In this paper, a new focal quality indicator, the 2D-TKEO indicator, for the translational motion compensation is proposed. This indicator is based on the 2D Teager-Kaiser Energy Operator which represents the 'energy' of an image. In Inverse Synthetic Aperture Radar (ISAR) imaging of a non-cooperative target, the relative motion is unknown and it is therefore necessary to implement an autofocus approach to obtain high resolution imaging. This step is based on an optimization problem via the minimization of a cost function, thus making it possible to estimate the translational kinematic (speed, acceleration, jerk...) of the moving target. This paper describes the use of a new quadratic focal quality indicator to estimate the quality of an ISAR image. To validate our approach is presented on simulation results of a target constituted by ideal point scatterers models. The effectiveness of 2D-TKEO indicator is demonstrated on both noise-free and noisy simulations and results compared to current methods.**

***Index Terms*—2D Teager-Kaiser energy operator, Inverse Synthetic Aperture Radar, Translation motion compensation, Focal quality indicator.**

I. Introduction

In the last decades, the use of electromagnetic to image a moving target has been extensively considered in order to identify or to discriminate various objects (cars, aircrafts, ships, and so on). While the recent progress of ISAR imaging has been described in [1], [2]. The ISAR image formation revealed its limitation as it is related to the motion of a non-cooperative target. Indeed, generally unknown, it is necessary to estimate the relative movement of an object to obtain high quality ISAR images (in other words, to obtain focused ISAR images). This estimation will be all the more necessary if the movements of the target are complicated such as pitch, roll, or yaw motions [2], [3].

The kinematic of a target can be decomposed as translational and rotational motion. While the rotational kinematic of a target is necessary to obtain an ISAR image formation, the phase term associated to the translational kinematic (velocity, acceleration, and jerk) is the principal source of motion error and must be removed to obtain a highly focused ISAR image. The current methods to estimate the kinematics of a target are based on the motion compensation methods or autofocus algorithms. In the literature and various fields (biological microscopy, video, camera, radar...), wide of autofocus algorithms have been proposed to measure the degree of focus [1], [2], [4].

Indeed, the translational motion can be approximated with the Taylor polynomial model in radar imaging and the issue can be resolved as an optimization problem. Several techniques are therefore based on the use of image focus indicators such as contrast approach [5], entropy approach [6] and many others works. In this context, the main goal is understand how the new focal quality indicator, 2D-TKEO indicator, can be used in translational motion compensation.

We will perform such description as follow: in section II, we will first introduce the ISAR geometry, and describe the formation of the unprocessed ISAR spatial frequency spectrum of a target. We also present the translational motion compensation approach based on an optimization problem related to a definition of a focal quality indicator (or cost function). In the 3^{rd} section is described a new focal quality indicator based on the 2D Teager-Kaiser Energy Operator. Finally, we present numerical results and comments in section IV before conclusions and perspectives are addressed in the last section.

II. Signal Model

Based on the equations of Maxwell, the electromagnetic back-scattering mechanisms can be complicated for complex targets. However, the point-scatterer model can be used to simply characterize the received Radar Cross-Section (RCS) signal of a moving target [1]–[3]. In this model, the target is modeled as a set of localized point-scatterers, the total number is K (such as equation 2). Furthermore, the target is at the far field of the radar and the distance between the radar and the target is bigger than the dimensions of the object.

The movement of the target are described by a translational and rotational motion relative to the radar. Thus, $r(t)$ describes the translational position of the target's center of mass relative to the radar, and $\theta(t)$ is the rotational position of the target relative to xy (Fig. 1).

The transmitted signal of radar is a stepped-frequency continuous waveform (SFCW) consisting of M bursts; with each burst containing N pulses (Fig. 2). It should be noted that the radar Line-Of-Sight (LOS) is fixed during each burst.

The backscattered signal received by the radar receiver can be represented as the sum of each localized point-scatterers of the object as follow:

$$S(n,m) = e^{-\frac{4i\pi f_n r_{n,m}}{c}} H(n,m) + \eta(n,m) \ , \qquad (1)$$

where $n = 0, ..., N-1$, $m = 0, ..., M-1$, c is the speed of light, and $\eta(n,m)$ is the additive complex white Gaussian noise of zero mean. Here, the two-dimensional (N by M matrix) complex array, $S(n,m)$, represents the unprocessed (uncompensated) ISAR spatial frequency spectrum of the target.

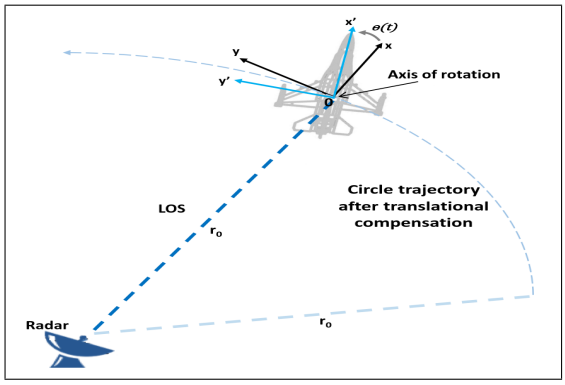

Fig. 1. ISAR Geometry of a rotating target.

The $H(n,m)$ target echo transfer function is the ideal translational motion compensated ISAR spatial frequency spectrum, and is given by:

$$H(n,m) = \sum_{k=1}^{K} \rho_k \; e^{-4i\pi \frac{f_n}{c}[x_k cos\theta_{n,m} + y_k sin\theta_{n,m}]} \;, \quad (2)$$

where (x_k, y_k) is the position of the k^{th} point-scatterer and ρ_k is the backscattered field amplitude of this point. The frequency, f_n, of the n^{th} pulse in a m^{th} burst is given by:

$$f_n = f_0 + n\delta f \;, \quad (3)$$

where f_0 is the frequency of the first pulse and δf is the frequency step from pulse to pulse.

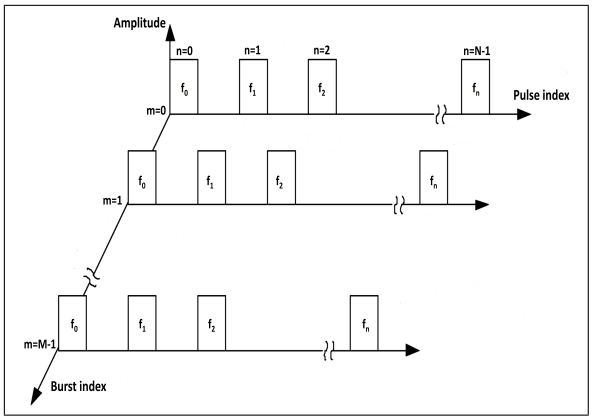

Fig. 2. Representation of SFCW radar signal.

The equations for translational and rotational movements of the object at a specific time point is illuminated by the $(n,m)^{th}$ pulse and can be defined as:

$$r_{n,m} = r_0 + v_0 t_{n,m} + \frac{1}{2} a_0 t_{n,m}^2 + \frac{1}{6} j_0 t_{n,m}^3 \;, \quad (4)$$

where $r_{n,m}$ is the instantaneous target range, and (r_0, v_0, a_0, j_0) are the initial values of slant-range, velocity, acceleration, and jerk respectively.
Similarly:

$$\theta_{n,m} = \theta_0 + \omega_0 t_{n,m} + \frac{1}{2} \alpha_0 t_{n,m}^2 \;, \quad (5)$$

where $\theta_{n,m}$ is the instantaneous target angular displacement, and $(\theta_0, \omega_0, \alpha_0)$ the initial values of the angular displacement, velocity, and acceleration respectively.
The sampling time, $t_{n,m}$, is given by:

$$t_{n,m} = (n + mN)\delta t \;, \quad (6)$$

where δt is the time interval between adjacent pulses.

In principle, to reconstruct the ISAR image of the target, the conventional algorithms are based on the two-dimensional Fourier Transform (FT):

$$I(p,q) = \mathscr{F}_{2D} \{S(n,m)\} \;, \quad (7)$$

where $\mathscr{F}_{2D}$ denotes the two-dimensional Fourier Transform of $S(n,m)$, and $p = 0, ..., N-1$, $q = 0, ..., M-1$, and $|I(p,q)|$ is a range-Doppler matrix (ISAR image) that represents the reflectivity of the target.
It should be noted that the phase term $r_{n,m}$ in (Eq. 7) with (Eq. 1) and (Eq. 4) contained the quantities (r_0, v_0, a_0, j_0). The constant value r_0 has not really impacting on the imaging procedure. It assigns the centering of the target in the image without introducing any defocusing. An estimated value of r_0 can be selected easily to adjust the center of the target. By contrast, v_0, a_0, and j_0 give additional components called Doppler-shift error. This motion parameters cause degradation; distortions and blur that alter the appearance of the ISAR image (Fig. 9 and 10).

To reduce the distortions in the ISAR image, the principal objective of the translation motion compensation algorithm is to estimate the translational kinematic quantities $(\tilde{v}, \tilde{a}, \tilde{j})$ to obtain an estimate $\tilde{H}(n,m;\tilde{v},\tilde{a},\tilde{j})$ in (Eq. 2):

$$\tilde{H}(n,m;\tilde{v},\tilde{a},\tilde{j}) = S(n,m)F(n,m;\tilde{v},\tilde{a},\tilde{j}) \;, \quad (8)$$

where $F(n,m)$ function is obtained by:

$$F(n,m;\tilde{v},\tilde{a},\tilde{j}) = e^{+\frac{4i\pi f_n}{c}[\overbrace{\tilde{v}t_{n,m} + \frac{1}{2}\tilde{a}t_{n,m}^2 + \frac{1}{6}\tilde{j}t_{n,m}^3}^{\tilde{r}_{m,n}}]} \;, \quad (9)$$

with $\tilde{v}$, $\tilde{a}$, and $\tilde{j}$ the estimated motion parameters of a moving target: v_0, a_0, and j_0 respectively. After correction of the translation motion, the quality of the ISAR image is drastically improved, and the expression (Eq. 7) can be replaced by:

$$I(p,q) = \mathscr{F}_{2D} \left\{ \tilde{H}(n,m;\tilde{v},\tilde{a},\tilde{j}) \right\} \;. \quad (10)$$

As a result, the ISAR image estimated from (Eq. 10) will be more localized with less blurring. In fact, the precision of the translational kinematic quantities estimation is essential to

enhance the quality of ISAR image formation. As such, the next paragraph introduces a classical scheme to estimate the motion parameters $(\tilde{v}, \tilde{a}, \tilde{j})$.

Various ISAR autofocus approaches have been proposed [2], a few are based on the notion of image focus indicators such as matching pursuit [1], [7], contrast [5] and, entropy approaches [6]. These methods suppose that the translational kinematic of the target can be approximated by a polynomial model (see Eq. 4). The estimation of the parameters is then reduced to a relatively simple optimization. In our case, it is equivalent to a problem of minimizing (or maximizing[1]) a cost function, called focal quality indicator, including the three motion parameters as follows:

$$(\tilde{v}, \tilde{a}, \tilde{j}) = \underset{(v,a,j)\in\Omega}{\arg\min} \left\{ f_{cost}(v, a, j) \right\} \ , \tag{11}$$

with $f_{cost}(.)$ the cost function, $\Omega = \{V, A, J\}$, and (V, A, J) the search spaces of $(\tilde{v}, \tilde{a}, \tilde{j})$ values respectively with $V = [\tilde{v}_{min}, \tilde{v}_{max}]$, $A = [\tilde{a}_{min}, \tilde{a}_{max}]$, and $J = [\tilde{j}_{min}, \tilde{j}_{max}]$.
It should be noted that the variables are discrete. The expression (Eq. 11) therefore describes a discrete optimization problem and can be resolved using an exhaustive search (brute force approach). Of course, there are various optimization techniques to effectively resolve this problem such as algorithms based on Gradient approaches, Nelder-Mead algorithm [8], or Genetic algorithm [9].

III. Radial Motion compensation using 2D Teager-Kaiser Energy Operator

In the 1990s, Kaiser and *al.* proposed to compute the energy of a system using Teager-Kaiser Energy Operator (TKEO) [10]. Despite its simple definition (Eq. 15), this quadratic operator is used in many field of signal processing such as Time-Frequency analysis [11] and, demodulation of AM-FM signals [12] ... Some various generalizations have also been recently proposed such as for complex-valued signals [13], [14], and also for two dimensions image both real-valued [15]–[18] or complex-valued [19].

The 2D Teager-Kaiser Energy Operator TKEO, 2D-TKEO, is close to a local mean weighted 2D-Laplacian-filter and is defined as:

$$\Psi_{2\mathbb{R}}[I] \triangleq \|\nabla I\|^2 - I\Delta I \ , \tag{12}$$

where $I \equiv I(x, y)$ is a real-valued 2D image, (x, y) are the spatial coordinates of the pixel. ∇ and $\Delta{=}\nabla^2$ stand for the gradient and the Laplacian respectively:

$$\|\nabla I\|^2 = \left(\frac{\partial I}{\partial x}\right)^2 + \left(\frac{\partial I}{\partial y}\right)^2 \ , \ \Delta I = \frac{\partial^2 I}{\partial x^2} + \frac{\partial^2 I}{\partial y^2} \tag{13}$$

From this definition, it follows directly that:

$$\Psi_{2\mathbb{R}}[I] = \Psi_{\mathbb{R}}[I](x) + \Psi_{\mathbb{R}}[I](y) \ , \tag{14}$$

[1]to maximize $f_{cost}(.)$ is equivalent to minimize the negation of $f_{cost}(.)$

where $\Psi_{\mathbb{R}}[I](x)$ (or $\Psi_{\mathbb{R}}[I](y)$) is a classical form of Teager-Kaiser Energy Operator of 1D signal $f(t)$:

$$\Psi_{\mathbb{R}}[f](t) \triangleq \left[\dot{f}(t)\right]^2 - f(t)\ddot{f}(t) \ , \tag{15}$$

$\Psi_{2\mathbb{R}}[I]$ is a sum of each 1D energy component applied along the two directions x and y. By extending few of its properties:

$$\begin{aligned}
\Psi_{2\mathbb{R}}[I+J] &= \Psi_{2\mathbb{R}}[I] + \Psi_{2\mathbb{R}}[J] - J\Delta I - I\Delta J + 2\nabla I.\nabla J \\
\Psi_{2\mathbb{R}}[IJ] &= I^2\Psi_{2\mathbb{R}}[J] + J^2\Psi_{2\mathbb{R}}[I] \\
\Psi_{2\mathbb{R}}[cI] &= c^2\Psi_{2\mathbb{R}}[I] \\
\Psi_{2\mathbb{R}}[I+c] &= \Psi_{2\mathbb{R}}[I] - c\Delta I \\
\Psi_{2\mathbb{R}}[c] &= 0
\end{aligned}$$

where c is a constant image, and I, J real images. The symbol $'.'$ denotes inner product. The next paragraph introduces a common method to estimate a discrete version of $\Psi_{2\mathbb{R}}[I]$.

For a discrete image $I(p,q)_{0\leq p\leq(N-1),\ 0\leq q\leq(M-1)}$, the expression (Eq. 12) becomes:

$$\begin{aligned}
\Psi^A_{2\mathbb{R}}[I(p,q)] = {} & 2I^2(p,q) - I(p-1,q)I(p+1,q) \\
& - I(p,q-1)I(p,q+1) \ .
\end{aligned} \tag{16}$$

This equation (Eq. 16) is obtained by applying the one-sample difference operation along both the vertical and the horizontal directions. Note that this is only one among many suitable techniques used to obtain a discrete version of $\Psi_{2\mathbb{R}}[I]$. Another extension can be obtained along diagonal directions:

$$\begin{aligned}
\Psi^B_{2\mathbb{R}}[I(p,q)] = {} & 2I^2(p,q) - I(p-1,q+1)I(p+1,q-1) \\
& - I(p-1,q-1)I(p+1,q+1) \ .
\end{aligned} \tag{17}$$

As a result, the energy of an image I at location (p, q) can be determined by:

$$\Psi_{2\mathbb{R}}\left[I(p,q)\right] = \max\left(\Psi^A_{2\mathbb{R}}[I(p,q)],\ \Psi^B_{2\mathbb{R}}[I(p,q)]\right) \ . \tag{18}$$

This $\max(.)$ operator reflects more precisely the local activity of the pixel rather than, for example, the amplitude of the gradient [18], [19].

Finally, it is possible to define a new focal quality indicator, 2D-TKEO indicator, based on $\Psi_{2\mathbb{R}}[.]$, applied to the ISAR image:

$$(\tilde{v}, \tilde{a}, \tilde{j}) = \underset{(v,a,j)\in\Omega}{\arg\min} \left\{ -\sum_{p=0}^{N-1}\sum_{q=0}^{M-1} \Psi_{2\mathbb{R}}\left[\bar{I}(p,q;v,a,j)\right] \right\} \ , \tag{19}$$

where the power normalized ISAR image is defined as:

$$\bar{I}(p,q;v,a,j) = \frac{|I(p,q;v,a,j)|^2}{\sum_{p=0}^{N-1}\sum_{q=0}^{M-1}|I(p,q;v,a,j)|^2} \ , \tag{20}$$

and $I(p,q;v,a,j)$ is the ISAR spectrum using the 2D-Fourier Transform of $\tilde{H}(n,m;v,a,j)$ (Eq. 10). Note that this is only one among other possible expressions and another extension can be obtained based on a maximum or even a standard deviation form.

IV. Results

In this section, several simulations are presented in order to evaluate the performances of ISAR imaging after compensation of translation motion based on 2D-TKEO indicator (Eq. 19).

In all our simulations, the geometry of the airplane is depicted Fig. 3. This synthetic target is the MIG25 dataset described in [2] which consists of 120 point scatterers of equal reflectivity. For clarity, the simulation parameters of radar and target are reported table I. The values of N and M are set at 256 to ensure that figures (Fig. 9, 10, and 11) better reflect the potentials of the method. We use an exhaustive optimization procedure over a three dimensional (v, a, j) search space confined to the region $V = [-6.02, -2.02]m/s$, $A = [13.2, 15.2]m/s^2$, and $J = [-0.05, 0.15]m/s^3$.

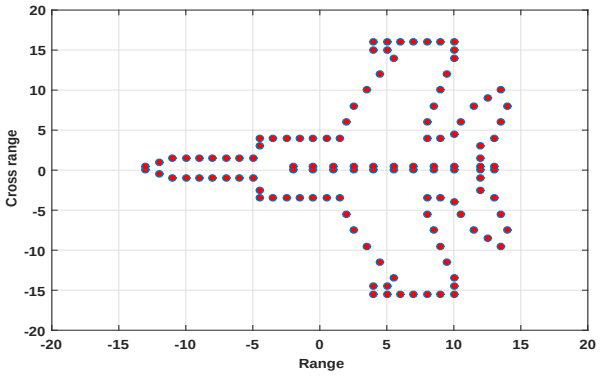

Fig. 3. Geometry of the target.

Figure 4 shows the results of the exhaustive search based on the cost function of 2D-TKEO indicator. The convexity near the center of the search space corresponds to the position of the minimum. Figure 5 shows translational velocity, acceleration, and jerk slices through the 2D-TKEO indicator surface described in equation (19). The green vertical curve in these subplots show the true values. Clearly, optimization techniques can be used to find the translation motion parameters that correspond to the global minimum.

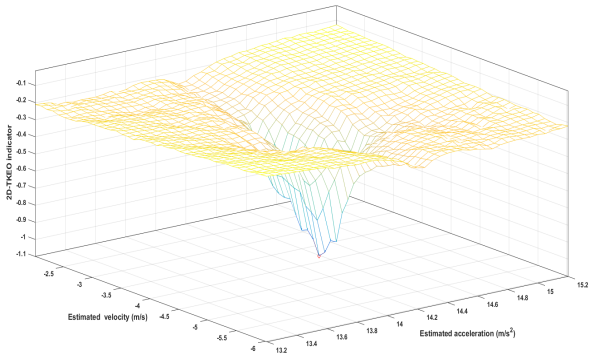

Fig. 4. Cost function of 2D-TKEO indicator with translational jerk $j = 0.05m/s^3$.

TABLE I
Radar and target parameters.

Parameter name	Symbol	Value
Number of pulses	N	64 (256)
Number of Burst	M	64 (256)
Step frequency	δf	2.13 MHz
Initial frequency	f_0	0.372 GHz
Pulse Repetition Interval	δt	1.59 ms
Translational kinematic $[m, m/s, m/s^2, m/s^3]$	$[r_0, v_0, a_0, j_0]$	$[4400, -4.02, 14.2, 0.05]$
Rotational kinematic $[rad, rad/s, rad/s^2]$	$[\theta_0, \omega_0, \alpha_0]$	$[1.58, 0.057, 1.8e^{-4}]$

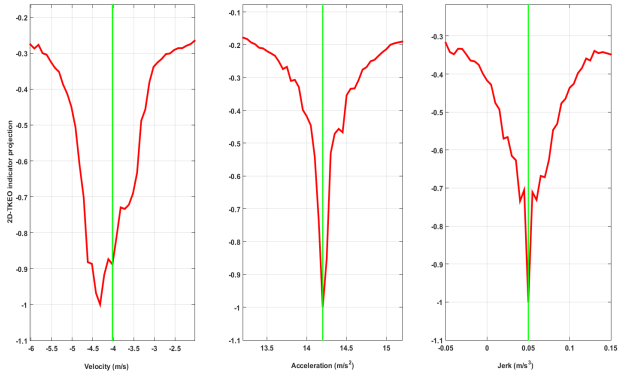

Fig. 5. Translational velocity, acceleration, and jerk surface slices.

For comparing the 2D-TKEO indicator approach with matching pursuit, contrast and entropy methods, the simulations have been corrupted by additive complex white Gaussian noise (Eq. 1). To characterize the performances, a total of 500 trials have been used for each SNR value, and associated Root Mean Square Error (RMSE) and Mean Absolute Error (MAE) are computed. RMSE and MAE are defined as:

$$RMSE = \sqrt{\frac{1}{W}\sum_{w=1}^{W} |\tilde{x}_w - x_w|^2}\ , \tag{21}$$

$$MAE = \frac{1}{W}\sum_{w=1}^{W} |\tilde{x}_w - x_w|\ , \tag{22}$$

where W is the number of Monte-Carlo simulation (here W is set as 500), $\tilde{x}$ is the prediction and x is the true value.

From figures 6, 7, and 8, the proposed approach performs better than matching pursuit method. When comparing to the two others approaches (contrast and entropy), the new method is nearly equivalent except that the 2D-TKEO indicator computes less outliers values (Fig. 6). From both figures 7 and 8, it should be noted that the computed curves (RMSE and MAE) based on entropy and contrast methods are superimposed.

Although the problematic of the rotational motion compensation is not studied in this article, it is interesting to note that there are also many algorithms such as interpolation methods

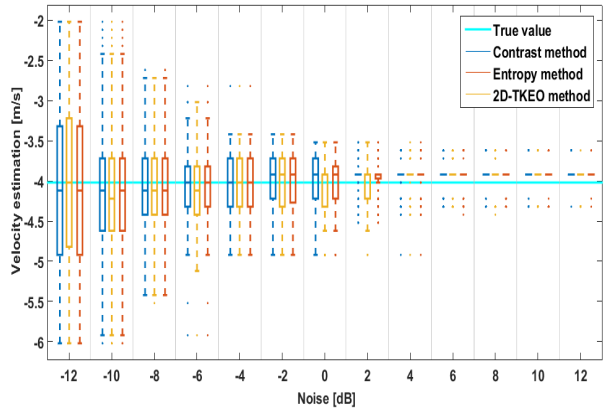

(a) Velocity estimation.

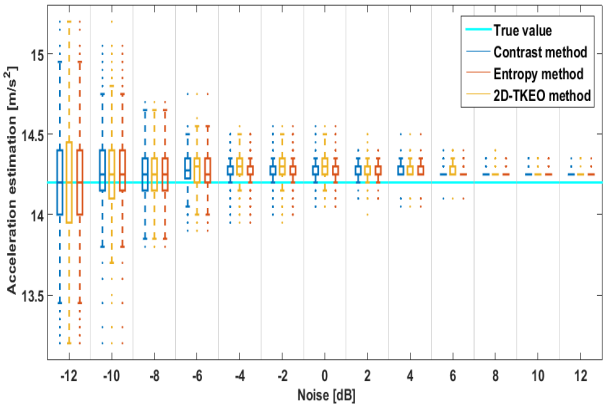

(b) Acceleration estimation.

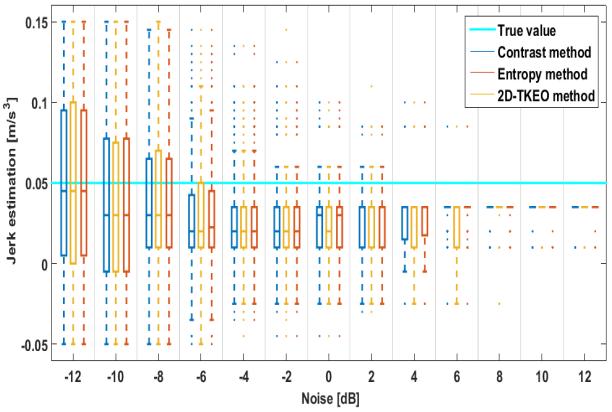

(c) Jerk estimation.

Fig. 6. Boxplots of the translational kinematic estimations.

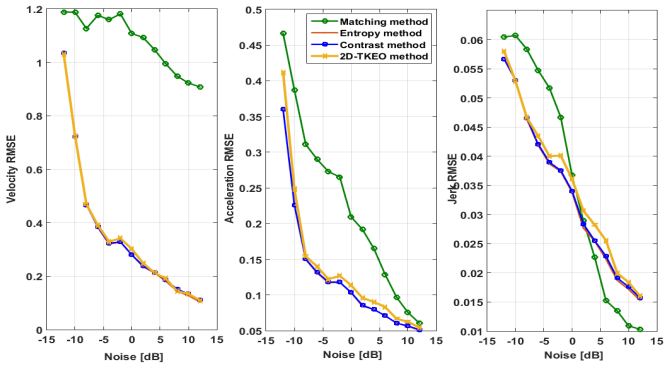

Fig. 7. RMSE comparison between various methods for the estimation of v(left), a(middle), and j(right).

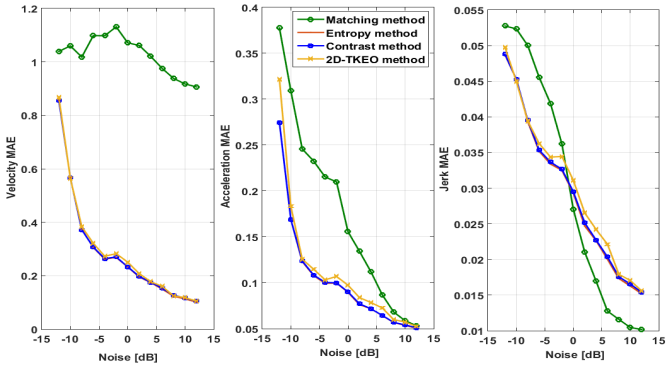

Fig. 8. MAE comparison between various methods for the estimation of v(left), a(middle), and j(right).

[2] and, Time-Frequency Transforms [3], [20]. Figures 11(a) and 11(b) show one frame ISAR image formation using Spectrogram and NSBEMD-TFD algorithm respectively. The NSBEMD-TFD is a new method based on Non uniformly Sampled Bivariate Empirical Mode Decomposition Time-Frequency Distribution [21]. From these simulation results, we can see that these approaches allow for the compensation of the rotational motion of a target.

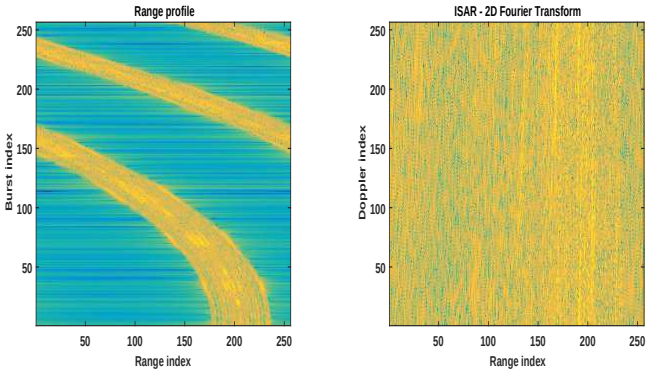

(a) Range profile. (b) ISAR using 2D-FT.

Fig. 9. Range profile and ISAR image of uncompensated target.

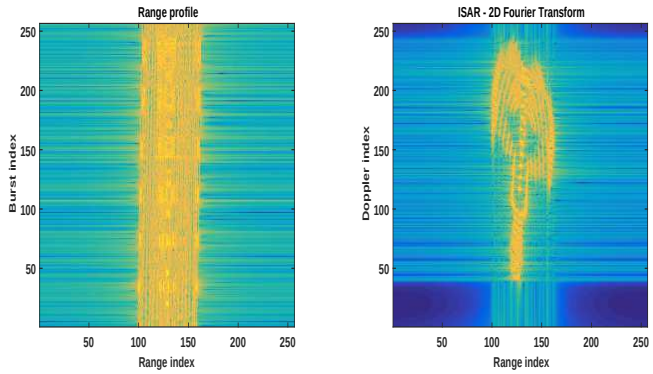

(a) Range profile. (b) ISAR using 2D-FT.

Fig. 10. Range profile and ISAR image of translation motion compensated target.

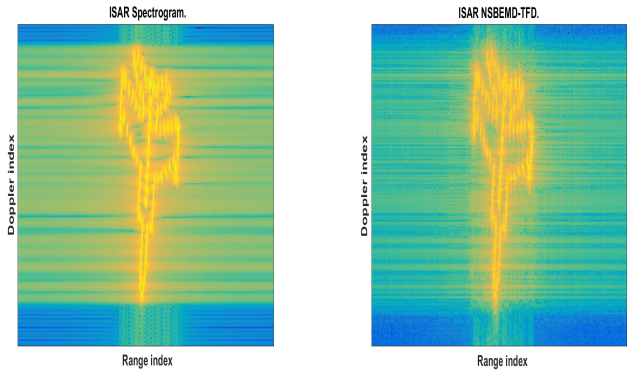

(a) ISAR using Spectrogram. (b) ISAR using NSBEMD-TFD.

Fig. 11. ISAR images using Time-Frequency methods after translation motion compensated target (frame 120).

V. Conclusions

In this paper, a new focal quality indicator based on Teager-Kaiser Energy Operator is used to estimate the translational kinematic of a moving target. The results show the validity of the approach proposed. The efficiency of ISAR imaging after the translational motion compensation is very interesting and is well adapted to non-stationary signals. To confirm the presented results, more simulations must be studied, preferentially using real dataset, and the results compared to other published algorithms.

References

[1] C. Ozdemir, *Inverse Synthetic Aperture Radar imaging with MATLAB algorithms*. John Wiley & Sons Publisher, 2012.

[2] V. C. Chen and M. Martorella, *Inverse Synthetic Aperture Radar Imaging - Principles, Algorithms and Applications*. SciTech Publishing, 2014.

[3] V. C. Chen and H. Ling, *Time-Frequency Transforms for Radar Imaging and Signal Analysis*. Artech House Publisher, 2002.

[4] F. C. Groen, I. T. Young, and G. Ligthart, "A comparison of different focus functions for use in autofocus algorithms," *Cytometry Part A*, vol. 6, no. 2, pp. 81–91, 1985.

[5] F. Berizzi and G. Corsini, "Focusing of two dimensional ISAR images by contrast maximization," *IEEE Microwave Conference, 1992. 22nd European*, vol. 2, pp. 951–956, 1992.

[6] L. Xi, L. Guosui, and J. Ni, "Autofocusing of ISAR images based on entropy minimization," *IEEE Transactions on Aerospace and Electronic Systems*, vol. 35, no. 4, pp. 1240–1252, 1999.

[7] G. Li, H. Zhang, X. Wang, and X.-G. Xia, "ISAR 2-D imaging of uniformly rotating targets via matching pursuit," *IEEE Transactions on Aerospace and Electronic Systems*, vol. 48, no. 2, pp. 1838–1846, 2012.

[8] J. A. Nelder and R. Mead, "A simplex method for function minimization," *The computer journal*, vol. 7, no. 4, pp. 308–313, 1965.

[9] M. Martorella, F. Berizzi, and S. Bruscoli, "Use of genetic algorithms for contrast and entropy optimization in ISAR autofocusing," *EURASIP Journal on Advances in Signal Processing*, vol. 2006, no. 1, p. 087298, 2006.

[10] J. F. Kaiser, "On a simple algorithm to calculate the 'energy' of a signal," *Acoustics, Speech, and Signal Processing, 1990. International Conference on*, pp. 381–384, 1990.

[11] J.-C. Cexus and A.-O. Boudraa, "Nonstationary signals analysis by Teager-Huang Transform (THT)," *IEEE Proc. European Signal Processing Conference, EUSIPCO'06*, pp. 1–5, 2006.

[12] P. Maragos, J. F. Kaiser, and T. F. Quatieri, "Energy separation in signal modulations with application to speech analysis," *IEEE transactions on signal processing*, vol. 41, no. 10, pp. 3024–3051, 1993.

[13] J.-C. Cexus and A.-O. Boudraa, "Link between cross-Wigner distribution and cross-Teager energy operator," *Electronics Letters*, vol. 40, no. 12, pp. 778–780, 2004.

[14] A.-O. Boudraa, S. Benramdane, J.-C. Cexus, and T. Chonavel, "Some useful properties of cross-ψ_B-energy operator," *AEU-International Journal of Electronics and Communications*, vol. 63, no. 9, pp. 728–735, 2009.

[15] T.-H. Yu, S. K. Mitra, and J. F. Kaiser, "Novel nonlinear filter for image enhancement," *Image Processing Algorithms and Techniques II*, vol. 1452, pp. 303–310, 1991.

[16] P. Maragos and A. C. Bovik, "Image demodulation using multidimensional energy separation," *JOSA A*, vol. 12, no. 9, pp. 1867–1876, 1995.

[17] F. Salzenstein, A.-O. Boudraa, and J.-C. Cexus, "Generalized higher-order nonlinear energy operators," *JOSA A*, vol. 24, no. 12, pp. 3717–3727, 2007.

[18] A.-O. Boudraa, A. Bouchikhi, and E.-H. S. Diop, "Teager-Kaiser energy bi-level thresholding," *Communications, Control and Signal Processing, 2008. 3rd International Symposium on*, pp. 1086–1090, 2008.

[19] J.-C. Cexus, A. Boudraa, A. Baussard, F. Ardeyeh, and E. Diop, "2D cross-ψ_B-energy operator for images analysis," *Communications, Control and Signal Processing, 2010. 4th International Symposium on*, pp. 1–4, 2010.

[20] B. A. H. Ahmed, J.-C. Cexus, and A. Toumi, "ISAR image formation with a combined Empirical Mode Decomposition and time-frequency representation," *IEEE Proc. European Signal Processing Conference, EUSIPCO'15*, pp. 1366–1370, 2015.

[21] O. Couderc, J.-C. Cexus, F. Comblet, A. Toumi, and A. Khenchaf, "ISAR imaging based on the Empirical Mode Decomposition Time-Frequency Representation," *Proc. International Radar Symposium 2016 - IRS'16*, pp. 1–5, 2016.